XV REUNIÓN NACIONAL CUATERNARIO
Bilbao 2019

GEOCHRONOLOGY OF THE CAVE SEDIMENTS AT GRAN DOLINA, ATAPUERCA (SPAIN): FROM IRON OXIDES TO HUMAN TEETH

J.M. Parés (1), M. Duval (2,1), D. Moreno (1), C. Álvarez (1), M. Sier (1), J. Rosell (3,4), J.M. Bermúdez de Castro (1), E. Carbonell, (3,4)

(1) Geología y Geocronología, CENIEH, Paseo Sierra de Atapuerca 3, 09002-Burgos, Spain.
(2) Australian Research Centre for Human Evolution, Environmental Futures Research Institute, Griffith University, 170 Kessels Road, Nathan, Australia.
(3) Institut Català de Paleoecologia Humana i Evolució Social, c/ Marcelí Domingo s/n, Campus Sescelades, 43007-Tarragona, Spain.
(4) Àrea de Prehistoria, Dept. d'Història de l'Art, Univ. Rovira i Virgili, Fac. de Lletres, Av. Catalunya, 35, 43002-Tarragona, Spain.
Department of Anthropology, University College London, 14 Taviton Street, London, WC1H 0BW, UK.

Resumen (título del trabajo): Geocronología de los sedimentos de cueva de Gran Dolina, Atapuerca: Desde óxidos de hierro a dientes humanos. *Se discuten datos existentes, y se presentan resultados nuevos sobre la geocronología de los sedimentos de relleno kárstico del yacimiento arqueo-palentológico de Gran Dolina, Atapuerca (Burgos). Los métodos utilizados incluyen el paleomagnetismo, resonancia paramagnética (ESR), luminiscencia, y Series del Uranio. En su conjunto, indican un relleno que se inicia alrededor de los 1.2 Ma y perdura hasta los 0.3 Ma aproximadamente. La presencia humana es patente a partir de los 900 Ka aproximadamente.*

Key words: Geochronology, paleoanthropology, Pleistocene, caves
Palabras clave: *Geocronología, paleoantropología, Pleistoceno, cuevas*

INTRODUCTION

Research at the Lower Paleolithic cave site of Gran Dolina, Sierra de Atapuerca (northern Spain) (Fig. 1), has led to major advances in our understanding of human evolution and occupation of Eurasia in the Pleistocene. The Gran Dolina site has produced thousands of fossils and artifacts since 1995, when the first hominin remains were reported, and soon became a Pleistocene landmark in studies of early human settlement outside the African continent (Carbonell et al., 1995; 2008). Stratigraphic layer TD6 of Gran Dolina has yielded over 170 human fossil remains, more than 200 lithic artifacts, classified as Mode 1, as well as several thousand small and large vertebrate remains (Bermúdez de Castro et al., 1997; Carbonell et al., 2005; Bermúdez de Castro et al., 2008; Ollé et al., 2013). The initial paleomagnetic dating at Gran Dolina revealed a switch from reverse to normal geomagnetic polarity above TD6 level, interpreted as the Matuyama-Brunhes boundary (MBB), providing a minimum age of 0.78 Ma for the archaeo-paleontological layer TD6 (Parés and Pérez-González, 1995). Subsequent chronometric analysis by Electron Spin Resonance (ESR) and luminescence further reinforced the paleomagnetic age (Falguères et al., 1999), and currently an age of around 0.85 Ma is accepted for the TD6 level (Parés et al., 2013; Arnold et al., 2014; Moreno et al., 2015). About four meters below TD6, stratigraphic layer TD4, a breccia of gravel-size clasts in a muddy and sandy matrix, is known to contain archaeological artifacts although no human fossils have been found yet (Carbonell and Rodriguez, 1994). The chronology of the ensemble TD4-TD5 levels is constrained by ESR dates on quartz grains and ranges between 0.9 to 1.13 Ma (Moreno et al., 2015). Such an age range overlaps with the Jaramillo Subchron (1.00-1.07 Ma) and therefore paleomagnetism allows testing whether level TD1 has an age older than 1.00 Ma, hence constraining the age of the overlying, lithic-tool bearing layer TD4.

There is very little chronological constraint on the underlying interior cave deposits that make up layer TD1, and even though is sterile, a better age for the sediments would constitute a maximum age for the overlying archeological layer. Since the MB boundary has been identified in TD7, TD1 is known to be older than 0.78 Ma (Parés et al., 2013). The only direct ages available so far are based on ESR dating of optically bleached quartz grains extracted from the top of TD1. The three samples dated by Moreno et al. (2015) confirm an Early Pleistocene chronology, but the age scatter (from 789$\pm$61 to 1249$\pm$126 ka) does not provide any further age constraint.

GEOLOGICAL SETTING

At first glance the Gran Dolina sedimentary deposits reveal a rather common succession in karstic tiered caves that developed in relation to progressive river incision. Passages of phreatic origin form at or just below the water table and are subjected to frequent flooding and associated deposition of slackwater deposits by stream flows. Accumulation of drip-type flowstones such as stalactites and stalagmites will often cap the fine clastic sediments, although these can also form after groundwater draining. In either case, the development of flowstones in caves has been associated with prolonged valley stability (e.g., Frank et al., 2006; Couchoud, 2008; Harmand et al., 2017). As incision lowers the local water table such passages are progressively abandoned and subjected to truncation by valley deepening, collapse, or fissuring that eventually will lead to the formation of a cave entrance. Talus, slope wash, and sliding bed mode deposits will then accumulate at the cave entrance and up to several meters in to the cave.

Such processes will produce a variety of gravel accumulation, diamictons, and channel facies, controlled by water availability and particle size (e.g., Bosh and White, 2004). The Gran Dolina stratigraphy has been divided into 12 main units termed TD1 to TD 11 from bottom to top (Campaña et al., 2017). It reflects a broad evolution and includes cave interior deposits at the bottom (including both silts, clays and flowstones) below TD4 unit, and an assemblage of diamictons and gravels often showing channel cut-and-fill structures with abundant sand and silts from TD4 to the top of the sequence. Cave entrance deposits will not be further considered in this paper and details can be found in Campaña et al. (2017). Below a prominent flowstone at the base of these cave entrance deposits (the basal “stalagmitic crust” of Carbonell and Rodríguez, 1994), the sedimentary record is mostly made up by silts and clays of fluvial origin (Fig. 2). Although a detailed study of such sediments is underway, the source of these cave interior sediments likely includes fluvial deposits and filtrates from soils (terra rossa). Silts and clays are often laminated, a quite common feature in phreatic environments (e.g., Ford and Williams, 2007), although the presence of two flowstones towards the top of the section suggests sporadic proximity to the vadose zone. The lower half of the stratigraphic section is characterized by a conspicuous unit of inclined laminar bedding silts and clays. Laminae are parallel to the depositional surface and therefore the unit corresponds to parallel accretion (Bull, 1981), so deposition of silt and clay laminae that are concordant to the underlying bedrock topography. Locally, such laminated silts and clays form couplets (3-4 cm thick), possibly suggestive of frequent flooding and drawing (Ford and Williams, 2007) by a mechanism linked to climatic events.

Consequently, our sampling was focused on both the cave interior deposits TD1-TD2, and the entrance facies TD4, TD5 and TD6.

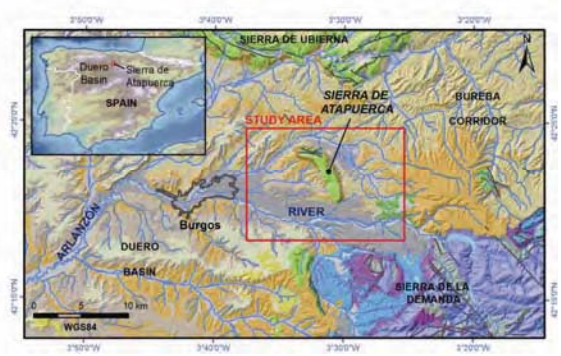

Fig. 1: Regional geological map of the study area showing the main lithological units (above), and a 3D view of the Atapuerca Mountain Range (Benito and Perez-Gonzalez, 2015).

RESULTS

As part of the sedimentary fabric study, the measurement of the AMS was carried out in the inclined laminar bedding silts and clays that appear in the lower part of the stratigraphic section. The distribution of the maximum axes of susceptibility show an overall tilt to the south and parallel to the measured dip of the laminae, whereas the minimum axes of susceptibility are normal to the lamination. Overall these observations are coherent with parallel accretion concordant to the dip of the underlying bedrock, and with the fluvial origin of this facies. Demagnetization diagrams show generally well behaved, stable remanent magnetization directions upon stepwise alternating field demagnetization. Many samples have a secondary low-coercivity component, possibly a viscous magnetization as the sediments have not been exhumed or thermally re-activated. Such low stability components are typically removed at fields of 15-20 mT and are apparent in samples where the high coercivity component has a negative inclination. The orientation of this viscous component typically conforms to that of the present day field at the locality and hence has not been further considered in our study. Taken together the demagnetization of the NRM and hysteresis curves suggest that PSD magnetite is present in the studied silts and clays, in agreement with our previous studies of sediments from the same cave system (Parés et al. 2016) and with numerous cave deposits elsewhere (e.g., Bosák et al., 2003; Rossi et al., 2016). The magnetostratigraphy of the sampled interval, expressed as the Virtual Geomagnetic Pole Latitude (VGP Lat) position, reveals that, for the most part, the cave interior deposits display reverse polarity. Data from the lowermost cave interior sediments are scarcer, due to the abundance of sandy silts that have produced either inconclusive or non interpretable demagnetization diagrams. A 100 cm-thick interval of normal polarity is observed at a depth between 2-3 m, and around a depth of 5.5 and 6.5 two shorter intervals of the same polarity as well. As far as ESR, the new results show an excellent goodness-of-fit (r^2>0.99), which contrast with the previous data (r^2<0.98) from Moreno et al (2015), resulting in a more reliable dose estimate and thus a more accurate age result. However, this ESR-Al age is far older than those obtained for TD1-08-01 and TD1-08-02. This may actually reflect some vertical variations of the sedimentary fluvial environment within the top of TD1 unit. The three ESR samples were indeed collected from two different facies observed within TD1, as defined by Campaña et al, (2017). We consider the Ti result as the most reliable estimate for the burial age of sample TD1-08-01bis. Last, the reconnaissance laser ablation data for U-Pb Geochronology, reveal typically low, and relatively constant, uranium concentrations around 50 ppb but with very large variations in Pb concentration from low ppb to high ppm values. Although areas with the highest U/Pb ratios (identified for analysis using laser ablation techniques) were sampled for the subsequent solution isotope dilution analyses, the U-Pb data reveal no discernable radiogenic ingrowth with increasing U/Pb ratios - at least within analytical uncertainties. As a result no U-Pb age information could be obtained for the two flowstones. At the present time therefore these materials remain undatable with traditional U-Pb isotope dilution methods. Research is however continuing into the development of in situ (laser ablation) dating methodologies which might ultimately allow the isolation of more radiogenic horizons suitable for age determination.

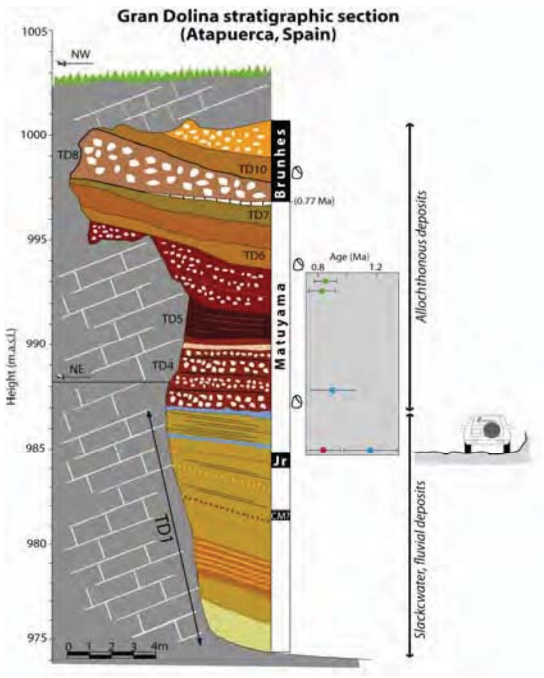

Fig. 2: Sedimentary infill at Gran Dolina site with magnetostratigraphic, OSL, and ESR results. Main lithostratigraphic units adapted from Campaña et al. (2015) and our own field observations. Notice the two main groups of sedimentary facies, including entrance (or allochthonous) facies deposits (TD4 through TD10) at the top, and slackwater, fluvial deposits (TD1) at the bottom, directly overlying the bedrock. In blue are shown the speleothems developed at the bottom unit TD1 (Parés et al., 2018).

CONCLUSIONS

The archaeological layers at Gran Dolina, including artifact-bearing level TD4, are preceded by about 9 meters of sterile, interior fluvial facies cave sediments that were deposited before the appearance of large openings to the cave (Fig. 2). The cave interior sediments are capped by a flowstone and followed by a pile of 15 meters of exterior facies sediments (talus, slope, sliding bed deposits), where fossil and artifact-bearing horizons are found. The age of the archaeological unit TD6 is constrain by a combination of paleomagnetism, ESR (both on quartz grains and on human teeth), and luminescence dates. The magnetic stratigraphy of the cave interior sediments reveals a dominant reverse magnetic polarity, coherent with a Matuyama age, and interrupted by a ca. 100 cm normal polarity magnetozone. Re-measured ESR ages on quartz grains in the upper part of TD1 produced an age range between 0.8 to 1.2 Ma, and therefore we interpret the shorth normal magnetozone as the Jaramillo Subchron (1.00-1.07 Ma). The oldest archaeological unit at Gran Dolina and artifact-bearing layer TD4 is overlying the studied layer TD1 and therefore post-dates the Jaramillo Subchron. The flowstone between units TD1 and TD4 (“stalagmitic crust”) indicate the proximity of the cavity to the vadose zone, and its formation shows a major change from interior facies (phreatic-vadose zone) to eventual cave entrances development, an environmental change that allowed the accumulation of slope, talus, and debris cones that contain the fossil and artefact horizons that make the Gran Dolina site so special.

Acknowledgements: Access and permission to collect samples in Atapuerca was granted by Junta de Castilla y León. The authors are deeply indebted to the Atapuerca Research Team (EIA) and the Fundación Atapuerca for continuous support of this research. Financial support for this work was obtained from Junta de Castilla y León and from MINECO Grants CGL2017-89603-R and CGL2015-65387-C3-3-P.

REFERENCES

Arnold, L. J., Demuro, M., Parés, J. M., Pérez-González, A**.**, Arsuaga, J. L., Bermúdez de Castro, J. M. & Carbonell, E., 2014, Evaluating the suitability of extended-range luminiscence dating techniques over early and Middle Pleistocene timescales: Published datasets and case studies from Atapuerca, Spain: *Quaternary International*, doi: 10.1016/j.quaint.2014.08.010.

Benito-Calvo, A. & Pérez-González, A., 2015. Geomorphology of the Sierra de Atapuerca and the Middle Arlanzón Valley (Burgos, Spain). *Journal of Maps*, 11, 535-544.

Bermúdez de Castro, J.M., Arsuaga, J.L., Carbonell, E., Rosas, A., Martínez, I., Mosquera, M. 1997. A hominid from the lower Pleistocene of Atapuerca, Spain: possible ancestor to Neandertals and modern humans. *Science* 276, 1392–1395.

Bermúdez de Castro, J.M., Pérez-González, A., Martinón-Torres, M., Gómez-Robles, A., Rosell, J., Prado, L., Sarmiento, S., Carbonell, E., 2008. A new early Pleistocene hominin mandible from Atapuerca-TD6, Spain. *Journal of Human Evolution*. 55, 729–735.

Campaña, I., Pérez-González, A., Benito-Calvo, A., Rosell, J., Blasco, R., Bermúdez De Castro, J.M., Carbonell, E., Arsuaga, J.L., 2016. New interpretation of the Gran Dolina-TD6 bearing Homo antecessor deposits through sedimentological analysis. *Scientific Reports*, 6: 34799; doi:10.1038/srep34799.

Campaña, I., Benito-Calvo, A., Pérez-González, A., Ortega, A.I., Bermúdez de Castro, J.M., Carbonell, E., 2017. Pleistocene sedimentary facies of the Gran Dolina archaeo-paleoanthropological site (Sierra de Atapuerca, Burgos, Spain). *Quaternary International* 433, 68-84.

Carbonell, E., and Rodríguez, X. P., 1994. Early-Middle Pleistocene deposits and artefacts in the Gran Dolina site (TD4) of the Sierra de Atapuerca (Burgos, Spain). *Journal of Human Evolution* 26: 291-311.

Carbonell, E., Bermúdez de Castro, J.M., Arsuaga, J.L. et al. 1995. Lower Pleistocene hominids and artifacts from Atapuerca-TD6 (Spain). *Science* 269, 826-829.

Carbonell, E., Bermúdez de Castro, J.M., Arsuaga, J.L., Allué, E., Bastir, M., Benito, A., Cáceres, I., Canals, T., Díez, J.C., Van der Made, J., Mosquera, M., Ollé, A., Pérez-González, A., Rodríguez, J., Rodríguez, X.P., Rosas, A., Rosell, J., Sala, R., Vallverdú, J., Vergés, J.M., 2005. An Early Pleistocene hominin mandible from Atapuerca-TD6, Spain. *Proceedings of the National Academy of Sciences of the United States of America* 102, 5674-5678.

Carbonell, E., Bermúdez de Castro, J.M., Parés, J.M., Pérez-González, A., Cuenca- Bescós, G., Olle, A., Mosquera, M., Huguet, R., van der Made, J., Rosas, A., Sala, R., Vallverdú, J., García, N., Granger, D.E., Martinón-Torres, M., Rodríguez, X.P., Stock, G.M., Vergès, J.M., Allué, E., Burjachs, F., Cáceres, I., Canals, A., Benito, A., Díez, C., Lozano, M., Mateos, A., Navazo, M., Rodríguez, J., Rosell, J., Arsuaga, J.L., 2008, The first hominin of Europe: *Nature*, v. 452, p. 465-470.

Couchoud, I., 2008. Les spéléothèmes, archives des variations paléoenvironnementales. *Quaternaire*, 19 (4) 255–274.

Cuenca-Bescós, G., Blain, H.A., Rofes, J., Lozano-Fernández, I., López-García, J.M., Duval, M., Galán, J., Núñez-Lahuerta, C., 2015. Comparing two different Early

Pleistocene microfaunal sequences from the caves of Atapuerca, Sima del Elefante and Gran Dolina (Spain): Biochronological implications and significance of the Jaramillo subchron. *Quaternary International*. 389, 148–158.

Duval, M. (2012). Dose response curve of the ESR signal of the Aluminum center in quartz grains extracted from sediment. Ancient TL 30(2): 1-9.

Duval, M. and Guilarte Moreno, V. (2012). Assessing the influence of the cavity temperature on the ESR signal of the Aluminum center in quartz grains extracted from sediment. Ancient TL 30(2): 11-16.

Duval, M. and Arnold, L. J. (2013). Field gamma dose-rate assessment in natural sedimentary contexts using LaBr3(Ce) and NaI(Tl) probes: A comparison between the “threshold” and “windows” techniques. Applied Radiation and Isotopes 74(0): 36-45.

Duval, M., Sancho, C., Calle, M., Guilarte, V., Peña-Monné, JL., 2015. On the interest of using the multiple centers approach in ESR dating of optically bleached quartz grains: some examples from the Early Pleistocene terraces of the Alcanadre River (Ebro basin, Spain). *Quaternary Geochronology* 29, 58-69.

Duval, M., Arnold, L. J., Guilarte, V., Demuro, M., Santonja, M. and Pérez-González, A. (2017). Electron spin resonance dating of optically bleached quartz grains from the Middle Palaeolithic site of Cuesta de la Bajada (Spain) using the multiple centres approach. Quaternary Geochronology 37: 82-96.

Falguères, C., Bahain, J.J., Yokoyama, Y., Arsuaga, J.L., Bermúdez de Castro, J.M., Carbonell, E., Bischoff, J.L., Dolo, J.M., 1999. Earliest humans in Europe: the age of TD6 Gran Dolina, Atapuerca, Spain. *Journal of Human Evolution* 33, 343-352.

Ford, D., and Williams, 2007. *Karst Hydrogeology and Geomorphology*, John Wiley & Sons, Ltd.

Grün, R., 1994. A cautionary note: use of the water content and depth for cosmic ray dose rate in AGE and DATA programs. *Ancient TL* 12, 50-51

Harmand, D., Adamson, K., Rixhon, G., Jaillet, S., Losson, B., Devos, A., Hez, G., Calvet, M., Audra, P., 2017. Relationships between fluvial evolution and karstification related to climatic, tectonic and eustatic forcing in temperate regions, *Quaternary Science Reviews*, http://dx.doi.org/10.1016/j.quascirev.2017.02.016

Moreno, D., Falguères, C., Pérez, A., Voinchet, P., Ghaleb, B., Despriée, Bahain, J.J., Sala, R., Carbonell, E., Bermúdez de Castro, J.M., Arsuaga, J.L. 2015. New radiometric dates on the lowest stratigraphical section (TD1 to TD6) of Gran Dolina site (Atapuerca, Spain). *Quaternary Geochronology* 30, 535-540.

Ollé, A., Mosquera, M., Rodríguez, X.P., de Lombera-Hermida, A., García-Antón, M.D., García-Medrano, P., Peña, L., Menéndez, L., Navazo, M., Terradillos, M., Bargall_o, A., Márquez, B., Sala, R., Carbonell, E., 2013. The Early and Middle Pleistocene technological record from Sierra de Atapuerca (Burgos, Spain). *Quaternary International* 295, 138-167.

Ortega, A.I., Benito-Calvo, A., Pérez-González, A., Martín-Merino, M.A., Pérez-Martínez, R., Pares, J.M., Aramburu, A., Arsuaga, J.L., Bermúdez de Castro, J.L., Carbonell, E., 2013. Evolution of multilevel caves in the Sierra de Atapuerca (Burgos, Spain) and its relation to human occupation. *Geomorphology*, v.196, p. 122–137.

Ortega, A.I., Benito-Calvo, A., Pérez-González, A., Arsuaga, J.L., Bermúdez de Castro, J.L., Carbonell, E., 2014. Atapuerca Karst and its Palaeoanthropological Sites. In F. Gutiérrez and M. Gutiérrez (eds.), *Landscapes and Landforms of Spain*, World Geomorphological Landscapes, Springer Science+Business Media Dordrecht 2014, pp. 101-111.

Parés, J.M.; Álvarez, C.; Sier, M.; Moreno, D., Duval, M.; Woodhead, J.D.; Ortega, A.I.; Campaña. I., Rosell, J.; Bermúdez de Castro, J.M.; Carbonell, E., 2018. Chronology of the cave interior sediments at Gran Dolina archaeological site, Atapuerca (Spain). Quat. Sci. Rev., 168:1-16.

Parés, J.M. & Pérez-González, A. 1995. Paleomagnetic age for hominid fossils at Atapuerca Archaeological site, Spain. *Science* 269: 830-832.

Parés, J.M., Pérez-González, A., Arsuaga, J.L., Bermúdez de Castro, J.M., Carbonell, E., Ortega, A., 2010. Characterizing sedimentary history of cave deposits, using archaeomagnetism and rockmagnetism, Atapuerca (N Spain), *Archaeometry* 52, 5: 882–898.

Parés, J.M., Lee., A., Duval., M., Demuro, D., Pérez-González, A., Bermúdez de Castro, J.M., Carbonell, E., and Arsuaga, J.L., 2013. Reassessing the age of Atapuerca TD-6 (Spain): New paleomagnetic data, *Journal of Archaeological Sciences* 40, 4586–4595.

Parés, J.M., Ortega, A.I., Benito-Calvo, A., Aranburu, A., Arsuaga, J.L., Bermúdez de Castro, J.M., and Carbonell, E., 2016, Paleomagnetic constraints on the Atapuerca karst development (N Spain), In: Feinberg, J., Gao, Y., and Alexander, E.C., Jr., eds., *Caves and Karst Across Time*: Geological Society of America Special Paper 516, p. 285–300; doi:10.1130/2016.2516(22).